Estuaries and Coasts (2011) 34:90–105
DOI 10.1007/s12237-010-9324-z

The Shaping of An Estuarine Superfund Site: Roles of Evolving Dynamics and Geomorphology

Robert J. Chant · David Fugate · Ed Garvey

Received: 28 August 2009 / Revised: 20 March 2010 / Accepted: 15 June 2010 / Published online: 10 September 2010

Abstract Analysis of moored and shipboard hydrographic data along with suspended sediment data is used to provide the first comprehensive description of the dynamics and sediment transport processes of the Passaic River. The river has been highly depositional since dredging ceased in the 1940s and within this sedimentary record are high levels of contaminants including high levels of dioxins. Moored current meter data indicates that during low freshwater discharge both tidal period and residual flows favor a landward sediment flux. In contrast during moderate to high river flows the salt field is washed out of the system and results in a net downstream sediment flux that overcome the more persistent but weaker upstream flux during low river flow conditions. Consequently, with today's channel morphology the Passaic exports sediment to Newark Bay that we estimate is approximately equal the annual loadings. This, together with historical bathymetric surveys, suggests that the channel is approaching geomorphological equilibrium. Bathymetric changes in the Passaic River over the past 60 years have significantly altered the river's ability to trap sediments and contaminants and are consistent with the fact that most of the dioxins released to the river in previous decades appear to be trapped within the channel, despite the fact that they were released within a tidal excursion of the mouth. The decline in trapping efficiency is also consistent with a simple scaling analysis that suggests that the salt water intrusion length, and thus the ability to trap sediment, scales with the cube of the channel depth. Consequently, as the estuary shoaled its ability to trap sediments and contaminants diminished rapidly.

Keywords Estuarine dynamics · Sediment transport · Geomorphology

R. J. Chant (✉)
Institute of Marine and Coastal Science, Rutgers University,
New Brunswick, NJ 08091, USA
e-mail: chant@marine.rutgers.edu

D. Fugate
Florida Gulf Coast University,
10501 FGCU Blvd,
Fort Myers, FL 33965, USA

E. Garvey
Malcolm Pirnie,
104 Corporate Park Dive, P.O. Box 851, White Plains, NY 10602,
USA

Introduction

In recent decades, water quality in the New Jersey/New York Harbor (Fig. 1) has improved significantly largely due to the implementation of the Clean Water Act. For example, since the 1970s fecal coliform levels in the harbor have dropped by several orders of magnitude and harbor-wide dissolved oxygen levels have risen significantly (Steinberg et al. 2004). Moreover, levels of many contaminants in the surficial sediments have also fallen by an order of magnitude over this period (Steinberg et al. 2004). However, below these relatively clean waters and surfical sediments lies the long history of industrialization. For example, mercury concentration in the surficial sediments today is 1–5 ppm but increases to 10–50 ppm in the underlying sediments (Steinberg et al. 2004). Sediment profiles of most other contaminants show a similar peak concentration below the sediment water interface and the depth of this peak depends on both the history of the loadings and the local sedimentation rate.

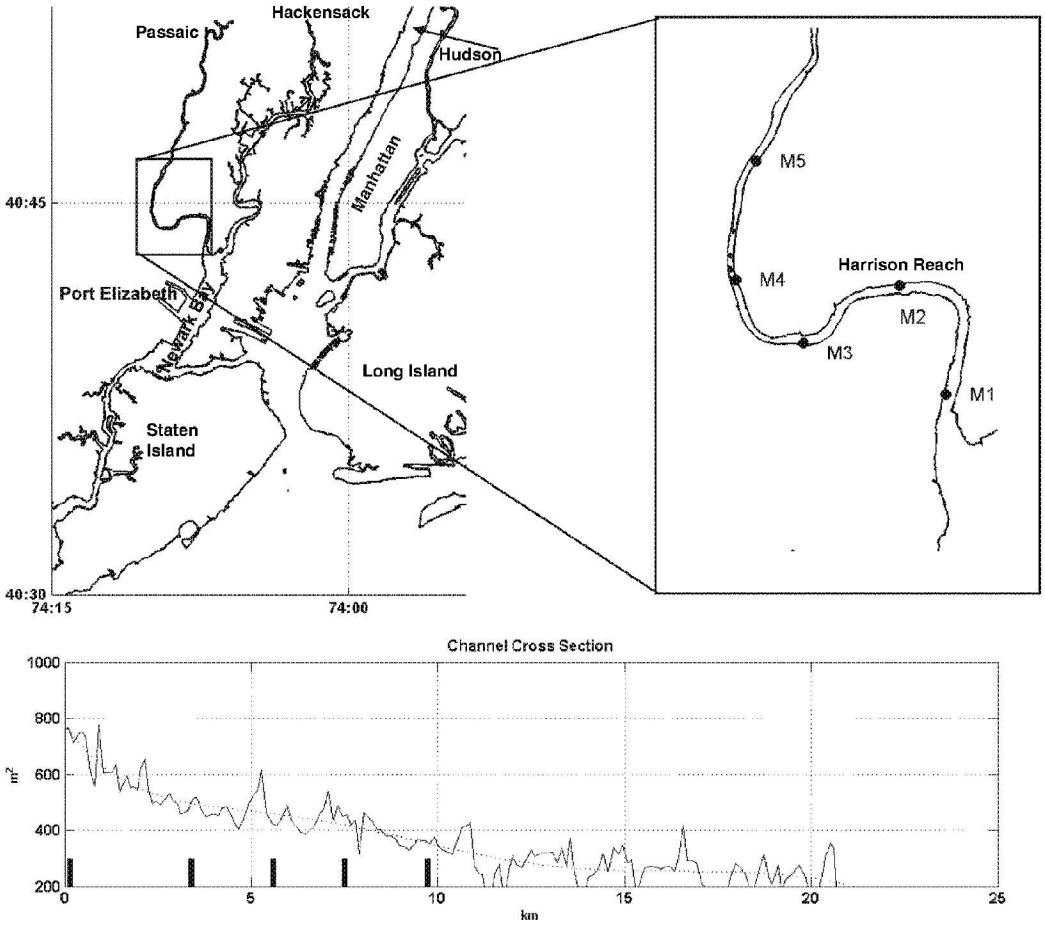

Fig. 1 Study site. Small scale map on *right* shows locations of moorings. The ADCP mooring that this study focuses on is at *M2*. *Lower panel* shows river cross-sectional area (*solid line*) along with smoothed estimate (*dashed*). *Thick vertical lines* show locations of moorings with *M1* to the *left* (~km 0) and *M5* to the *right* (~km 10)

Within the NY/NJ harbor lies the Passaic River (Fig. 1), which is perhaps the most contaminated system in the Harbor. The Passaic's industrial history dates back to colonial times when its power at the Great Falls in Patterson New Jersey was harnessed in a project conceived by Alexander Hamilton which put forth the Hamiltonian view of an American industrial society (Lurie and Mappen 2004). The ensuing intense industrial history in the Passaic's watershed is particularly intact in the lower 12 miles due to remarkably high sediment deposition rates over the past 60 years. The Harbor and its tributaries have been highly engineered to develop Port Newark/Elizabeth which lies just downstream of the Passaic River in Newark Bay (Fig. 1). Prior to this engineering Newark Bay was a broad shallow system with depths generally less that 2–3 m deep with a deeper channel 3–4 m deep leading into the Hackensack River and a 5–8 mdeep channel at its mouth leading into the Kill van Kull. The Harrison Reach of the Passaic River, which is the focus of this paper, is shown on the 1845 NOAA chart to have mean low water depths of approximately 3 m.

The engineering of this system commenced in the late nineteenth century and by 1940 the lowest 3–4 km of the Passaic River had been deepened to approximately 8–10 m, and to 6–7 m up to river km 10. However, with the construction of Port Elizabeth in 1940s dredging on the Passaic River ceased as port activities became focused downstream. Today the mean low water depths of the Passaic channel are approximately 4 m, although deeper holes of nearly 8 m exist in the vicinity of channel bends. Both historical charts and geochemical evidence (Huntley et al. 1995) indicate a sedimentation rate in the lower Passaic River of 5–10 cm/year over the past 60 years. During this highly depositional phase there has been intense

industrial development along the Passaic River and many of the contaminants associated with these industries are contained in the sediment record.

Among the contaminants buried in the Passaic are extremely high levels of 2,3,7,8-tetracholrodibenzo-p-dioxin (2,3,7,8 TCDD) associated with the manufacturing of Agent Orange that occurred in the lower Passaic between 1948 and 1974 (Bopp et al. 1991). Today a peak in dioxin levels lie 1–2 m below the sediment surface and this horizon is distributed evenly throughout the lower 12 miles of the River (Fig. 2). The well documented spike in cesium 137 indicates that the timing of this deposition was contemporaneous with the manufacturing of Agent Orange. While 2,3,7,8 TCDD levels at the surface are orders of magnitude lower than the subsurface peak, they are still above the United States Environmental Protection Agencies criteria "Effect Range-Medium." Moreover, a harbor-wide budget suggests the major contributor of 2,3,7,8 TCDD to the Harbor may be the remobilization of the Passaic River sediments (Powers et al. 2006).

This study focuses on the exchange of water and sediments between the Passaic River and Newark Bay. In particular, the study quantifies the role that tidal forcing, river flow, and estuarine circulation have on sediment transport processes. The transport of fine sediment in partially mixed estuaries is largely controlled by the interplay between stratification, turbulent mixing, resuspension, and the fall velocity of the suspended material (Geyer 1993; Dyer 1986, 1988). The feedback between the estuarine circulation, tidal velocities, and sediment transport processes ultimately shape the estuarine channel and may bring a system into geomorphological balance (Friedrichs and Aubrey 1995) (Friedrichs 1995) although continued natural and anthropogenic changes, such as sea level rise and bulkheading can drive continued morphodynamic evolution (Klingbeil and Sommerfield 2005).

Because estuarine sediment trapping is often dominated by frontal processes (Geyer 1993), a major objective of this study was to relate both estimates of sediment fluxes and salt water intrusion length to river discharge and tidal range. MacCready (1999) delineates estuarine parameter space with a fresh water Froude number (U_r/c) and a tidal Froude number (U_1/c), where U_r and U_1 are currents associated with the river flow and the tidal currents, respectively, and c internal wave speed $\sqrt{g'h}$ where h is the channel's depth and g' is reduced gravity and equal to $g\Delta\rho/\rho$ where g is gravity and $\Delta\rho$ and ρ are the density difference between the mouth and head of the estuary and the density of water, respectively. Note that both U_r and U_1 increase linearly with decreasing depth and thus we expect both Froude numbers to scale with $h^{-3/2}$ and thus as the channel shoaled over the past 60 years both Froude numbers have increased. Later, we will discuss how the shoaling has even stronger controls on salt water intrusion length and stratification, a tendency that is consistent with MacCready (1999) and that has significantly modified the sediment dynamics of this system.

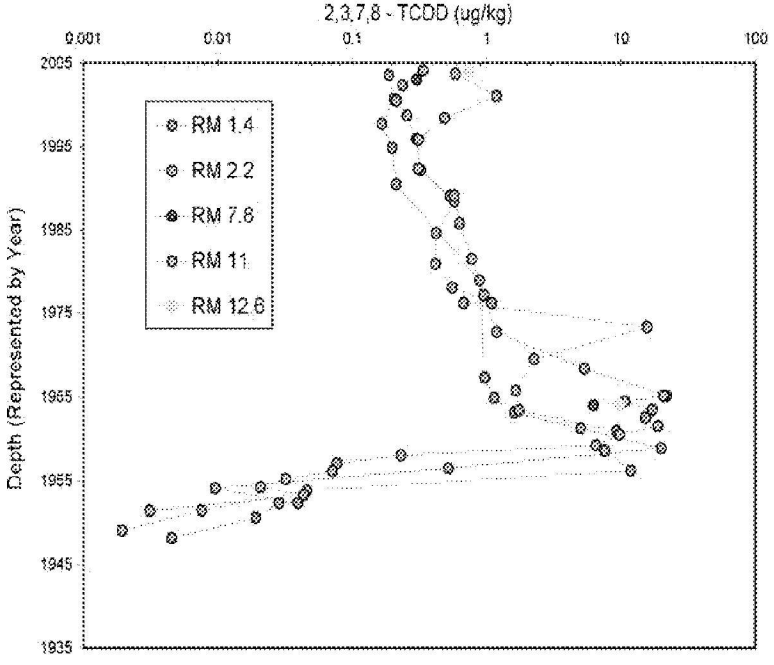

Fig. 2 Concentration of dioxin in sediment. Sediment date is based on Cs-137 concentration

In this paper, we place recent hydrographic measurements and estimates of sediment transport in context with the bathymetric change in the Passaic over the past 60 years. The observations were motivated by efforts to develop a plan to remediate this highly contaminated system and this study is the first intensive hydrodynamic study of this system. After describing the study site in the "Study Site" section and the field efforts in the "Field Program" section, we present results in the "Results" section that describe the structure of tidal and subtidal motion and characterize its variability as a function of river flow. We then characterize the response of the salt field to variations in river discharge and tidal forcing. These results facilitated an interpretation of the time varying suspended sediment transport which we decompose into tidal, riverine, and estuarine components in the "Sediment Transport" section. In the "Historical Infilling of the Passaic and Implications for 2,4,7,8 TCDD Trapping" section, an empirical sediment transport model is presented and discussed in terms of the implications on contaminant transport issues. Conclusions are drawn in the "Conclusions" section.

Study Site

The focus of the study is in the Harrison Reach of the Passaic River where Agent Orange was manufactured between 1948 and 1972 (Fig. 1). This reach of the Passaic River is approximately 1.5 km long and characterized by a sinuous channel with 90° bends upstream and downstream of the Harrison Reach. Today the channel is approximately 150 m wide and its cross section is laterally asymmetrical with a 4-m deep channel (MLW) close to the northern shore and a shallow shoal to the south. The river's cross-sectional area is 800 m^2 at the mouth and decreases to 500 m^2 around km 3.5 in the Harrison Reach (Fig. 1).

The Passaic River's watershed is 5,725 km^2, 80% of which lies upstream of the United States Geological Survey gauge at Little Falls in Patterson, New Jersey. This gauge has been operational since 1897 and the mean river discharge over entire record is 32 m^3/s. Maximum monthly mean discharge occurs in March (65 m^3/s) and minimum monthly mean discharge occurs July–September (15 m^3/s). River flows exceed 100 m^3/s nearly 6% of the time with the maximum recorded discharge of nearly 800 m^3/s occurring on October 10, 1903. These high river discharge events have significant impact on the estuarine dynamics and sediment transport processes as will be discussed later. Tides in the Passaic River are largely semidiurnal with a mean range of 1.5 m. The phase difference between tidal velocity and elevation is 90°, consistent with the dynamics of a shallow "equilibrium" tidal estuary (Friedrichs 2010).

Field Program

The field program consisted of shipboard surveys and moored instrumentation. The shipboard surveys consisted of profiling with a CTD/OBS package from Newark Bay to the head of salt with an along channel resolution of approximately 500 m. Moorings included a 1,200-kHz acoustic Doppler current profiler (ADCP) that was deployed at site 2 in the deep channel in the Harrison Reach along with a surface and bottom CT sensor. Four additional moorings containing surface and bottom CT sensors were deployed upstream and downstream of the Harrison Reach (Fig. 1). We note that the bottom CT sensors experienced serious fouling at in many of the deployments. The fouling appeared to be caused by debris (mostly plastic shopping bags) which were often found to be entangling the mooring frames upon recovery. There were three mooring deployments. The first two occurred during moderate to high river discharge and the third during low flow conditions. The timing of mooring deployment is also put in context with the river flow in Fig. 3 and summarized in Table 1. Both the optical backscatter obtained from the shipboard OBS profiling data and the acoustic backscatter from the moored ADCP were calibrated against suspended sediment concentrations.

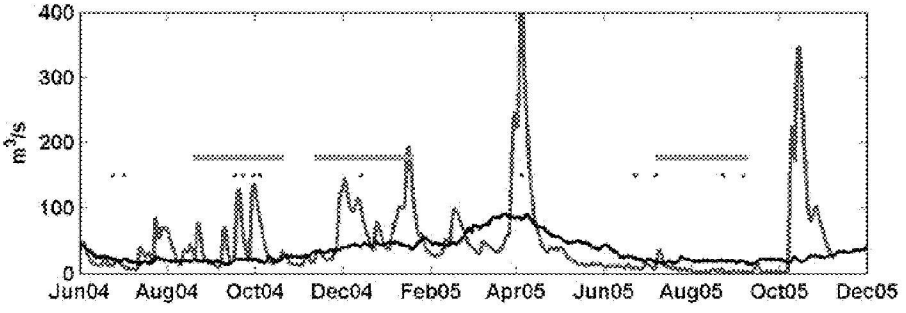

Fig. 3 River discharge during observational program (*blue line*) along with discharge climatology based on 110-year record at Little Falls (*Black Line*). *Red line* shows times of mooring deployment. *Blue dots* are times of CTD sections

Table 1 Timing of mooring deployment in context with the river flow

Deployment	Mean river discharge (m^3/s)	TSS flux rate (10^3 metric tons/year)	Tidal pumping (10^3 metric tons/year)	River flow (10^3 metric tons/year)	Estuarine shear (10^3 metric tons/year)
September 18, 2004–October 21, 2004	34	18	1.5	30	−13.7
October 19, 2004–January 19, 2005	63	115	70	94	−49.0
July 8, 2005–October 30, 2005	5	25	18	0.5	6.4

Results

Currents

Tidal Currents

Tidal motion in the Passaic is distorted by the non-linear generation of overtides and is flood dominated (Friedrichs and Aubrey 1988). During times of low river flow, the flood dominance is enhanced during spring tides; and depth averaged currents on flood are ~75 cm/s, while ebb currents are only 50–60 cm/s (Fig. 4a). These tidal asymmetries would lead to stronger bottom shear stresses on flood and act to transport sediment upriver. However, during times of high river discharge, ebb tides are significantly stronger than the flood. For high discharge events, the flood tide can be arrested (Fig. 4c) and this alone would drive a seaward sediment flux.

Tidal currents also exhibit tidal asymmetries in their vertical structure (Jay and Musiak 1993; Geyer et al. 2000; Chant and Wilson 2000) and are apparent in the mean velocity profile during the flood and ebb tide for each deployment (Fig. 5). During ebb tide, the flow is strongly sheared, while during the flood, shears are weaker; and there is some evidence of a subsurface velocity maximum, particularly during the high river flow conditions that occurred during the second deployment. Jay and Musiak (1993) pointed out that averaging these profiles over the tidal cycle (weak shear on flood and strong shear on ebb) results in a mean velocity profile that more closely resembles the ebb. If the river discharge is weak, this type of tidal asymmetry will yield a tidally averaged flow that is upstream at depth and downstream at the surface and in the same sense as the classic two-layer estuarine circulation (Hansen and Rattray 1966; MacCready 2004). More importantly, these profiles also emphasize a dramatic tidal asymmetry in near bottom velocity with significantly stronger currents on flood which would strongly favor a net upriver transport of sediment.

Estuarine Circulation

The estuarine circulation, or the mean flow, is clearly modified by river discharge (Fig. 6) and its vertical structure is similar to the ebb tide, suggesting the importance of tidal asymmetries in producing the mean circulation (Jay and Musiak 1993). During the third deployment, when the mean river discharge was 5 m^3/s, the mean flows exhibit the classic two-layer exchange with the lower layer flowing up river at ~5 cm/s and the upper

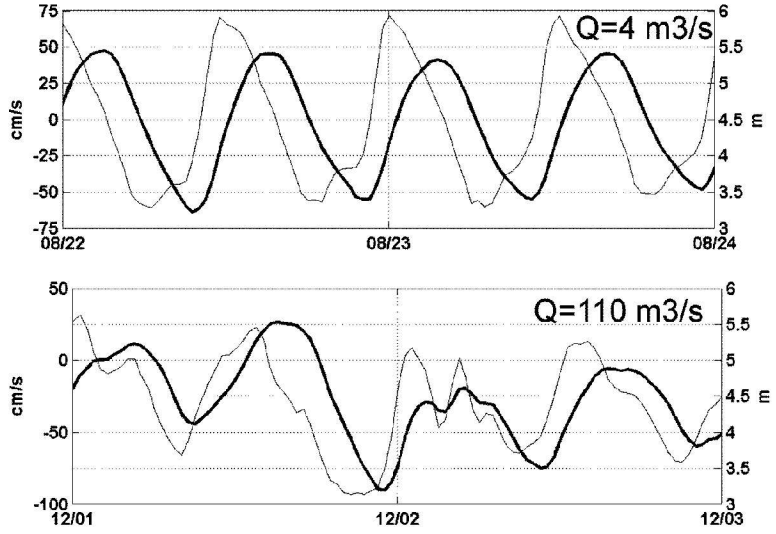

Fig. 4 Depth averaged currents (*thin line*) and tidal elevation (*thick line*) during a low flow condition (*upper panel*) and high flow conditions (*lower panel*) at site M2

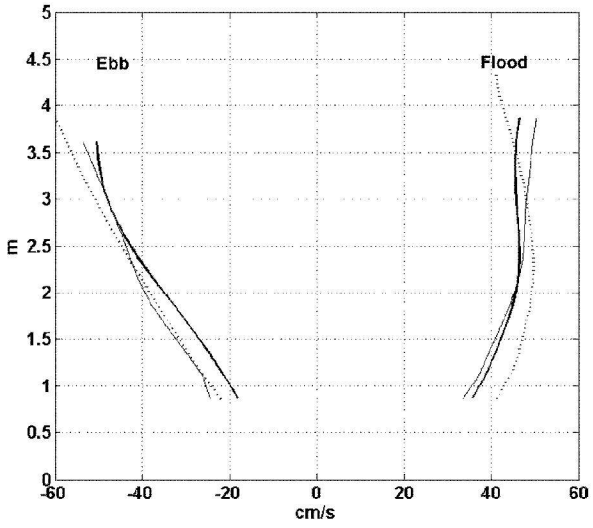

Fig. 5 Depth-dependent mean flow around peak flood and peak ebb for each of the three mooring deployments at site M2. *Thin solid line* for deployment 1, *thick solid line* for deployment 2, and *dashed line* for deployment 3

layer flowing seaward at approximately the same speed. However, during the first two deployments, when mean river discharges were 36 and 60 m^3/s, respectively, tidally averaged flows are mostly down river throughout the water column, with the exception of weak landward flows near the bottom during the second deployment. Vertical shears are strongest during the second deployment which had the highest mean river discharge, while shear was weakest during the first deployment with the lowest river discharge (Table 1).

Wind Forced Flows

Currents in the Passaic are also driven by winds and wind driven flows are apparent in the current meter records. The wind forced motion is primarily associated with remote forcing and is largely barotropic and highly correlated with nearby low-frequency sea level data. These fluctuations are on the order of 3–5 cm/s and are prominent in time series of low-frequency flows. However, they are an order of magnitude smaller than tidal currents or river-induced currents associated with large discharge events. Thus they appear to play a relatively minor role in the transport of sediment. Indeed, the correlation coefficient between low-frequency sea level and maximum daily stress only 0.08, while those associated with river discharge and tidal range are 0.5 and 0.7, respectively. While given the highly non-linear dynamics of sediment transport processes these meteorologically forced flows may play a larger role than indicated by their relationship to bottom stress, we neglect them in the following analysis because our results suggest that sediment transport processes in the Passaic are dominated by tides and river discharge with the latter being the dominant process driving sediment fluxes.

Salinity

The salt field responds strongly to both variations in river discharge and tidal forcing. During the first deployment, there were four river discharge events, the first two with discharges of approximately 50 m^3/s followed by two events of approximately 100 m^3/s (Fig. 7a). Note that the fouling of these sensors is evident in the data by times when tidal period fluctuations vanish, such as in mid-September at site 1 (Fig. 7a). For most of the deployment, the salt front moved downstream of mooring 3 during each ebb tide with the notable exception of low flow/neap tide conditions such as the neap tide in early September and again in early October. The salt field advanced past mooring 4 during these times (not shown). Unfortunately, near complete fouling of the sensor at site 5 during this deployment precludes determining when or if the salt field advanced past this mooring. Nevertheless, this spring/neap variability is suggestive of an upstream advance of the salt field during low flow neap tide conditions. During spring tides tidal period variability dominates the exchange flow and the salt front is advected further downstream on ebb. For example, as the tidal range increased between August 28 and September 1, the salt front was transported downstream of site 2 once each day during the stronger of the two daily tides. The second discharge event occurred during a weak neap tide and the salt front generally resided between sites 2 and 3 during the ebb. Nevertheless, these two events emphasize that for river flows of approximately

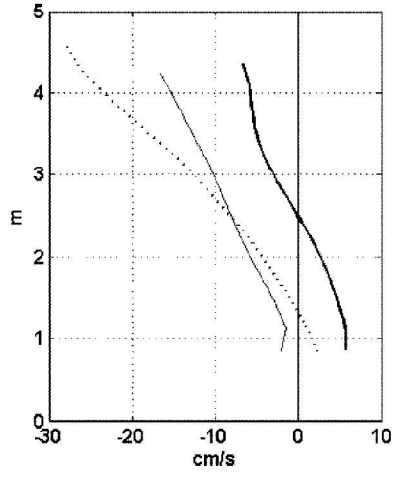

Fig. 6 Depth-dependent record mean for each of the three mooring deployments at site M2. *Thin solid line* for deployment 1, *thick solid line* for deployment 2, and *dashed line* for deployment 3

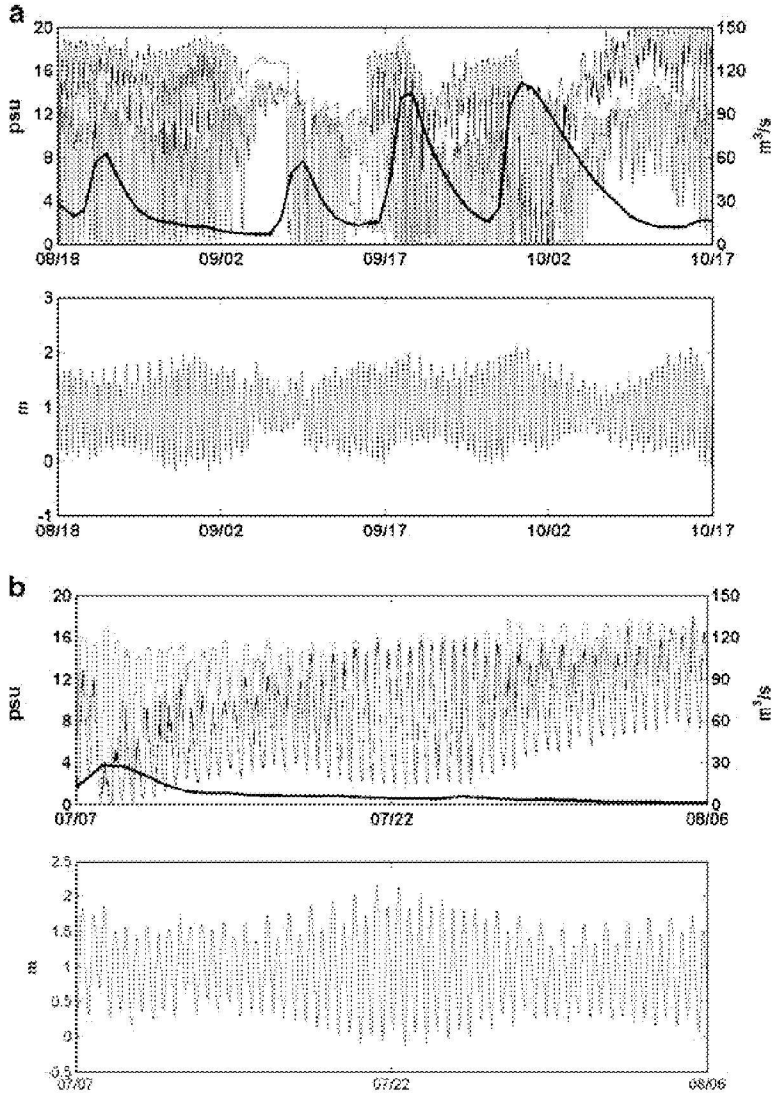

Fig. 7 **a** *Upper panel*. River discharge (*thick line*) and near bottom salinity at M3 (*blue line*), M2 (*red line*), and M1 (*black line*). *Lower panel* shows pressure record to emphasize spring/neap variability. **b** *Upper panel*. River discharge (*thick line*) and surface (*black*) and bottom (*red*) salinity from mooring M3. *Lower panel* shows pressure record to emphasizes spring/neap variability

50 m^3/s, the salt front resides in the vicinity of the Harrison Reach. During the two stronger events in mid-September and early October when river flow exceeded 100 m^3/s the salt front passed through the Harrison Reach each tidal cycle and completely out of the river during the last discharge event in early October.

River discharge was low during the third deployment and vertical stratification was marked by a dramatic spring/neap variability (Fig. 7b). During neap tide the top-to-bottom salinity difference approached 10 psu while the water column is well mixed during spring tides. This type of spring/neap variability is often observed in partially mixed estuaries (Geyer et al. 2000).

The response of the salt field to the river flow was also clearly evident in the shipboard surveys. Figure 8 shows the salt and total suspended sediment (TSS) fields from a low flow survey conducted in September 2005 when river discharge was 1 m^3/s and from a high flow event from April 5, 2005 when river flow was 330 m^3/s. During the low flow event, the 2 psu isohaline was 20 km upriver and the suspended load was characterized by a turbidity maximum in the vicinity of the head of salt with maximum suspended loads of 50 mg/l. In contrast during the high flow event the salt front was pushed out of the river and into Newark Bay. During this high flow event, total suspended sediment concentration approached 1 g/l and a plume of suspended sediment with concentrations of 50–100 mg/l is seen emanating from the Passaic River and into Newark Bay.

Finally, with each shipboard survey, we determined the along channel location of the near bottom 2 psu isohaline and plotted this as a function of river discharge (Fig. 9). We

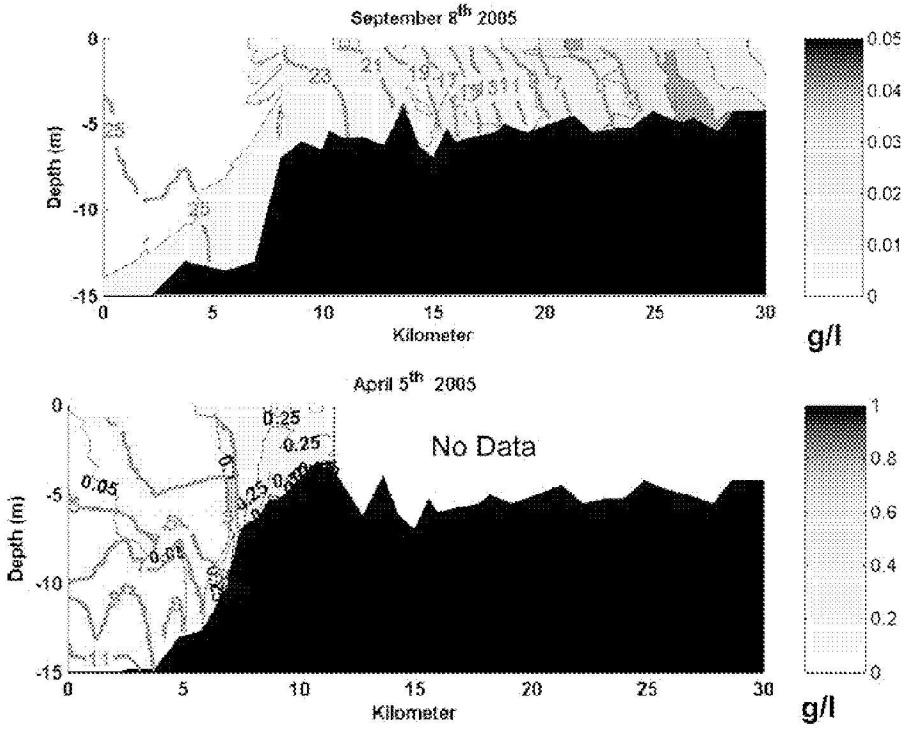

Fig. 8 Salinity and turbidity sections from CTD/OBS surveys of river during a low flow condition (*upper panel*) and high flow condition (*lower panel*). *Red contours* are salinity and *color* and *grey contours* represent suspended sediment in grams per liter. Note that there is a change in the suspended sediment scale between the low flow and high flow event. The mouth of the Passaic River is around km 8

note that these surveys were taken in approximately the same tidal phase beginning approximately 1 h after high water. Like the results from the moored data, the shipboard data shows that for river flows greater than 50 m^3/s the salt front resides in the vicinity of the Harrison reach. The best fit between the position of the 2 psu isohaline (X_2 in km) and the river discharge yielded (Q in m^3/s) yielded $X_2 = 12 \times Q^{-0.28}$. This fit is close to the theoretical relationship $X_2 \sim Q^{-0.33}$ between Q and X_2 (Hansen and Rattray 1966; Monismith et al. 2002; Ralston et al. 2008). However, the scaling assumes that the salt flux is dominated by the tidally mean quantities, which may not be the case here during high flow conditions when the system is frontal and exhibits significant time dependency. Nevertheless, while this "fit" may be fortuitous due to the limited data, it clearly indicates, as did the moored data, that the salt wedge resides within 1 tidal excursion (~7 km) from the mouth when the discharge is above 50–100 m^3/s, during which time tidal currents can sweep the salt front and the turbidity maximum out of the river and into Newark Bay.

Tidal Period Behavior of TSS

The nature of sediment transport processes at site M2 fundamentally differs between high and low flow events. For example, during the high flow event in late November 2004 near bottom salinity at site 2 dropped below 1 as the salt front was advected downstream of the mooring during the ebb on November 27 (Fig. 10a). The highest TSS levels occur as the salt front moves past the mooring during ebb late in the day on the 27th where TSS levels exceed 150 mg/l. TSS levels remain relatively low during the flood. This cycle of enhanced turbidity during the ebb tide persisted throughout the high flow event. In contrast

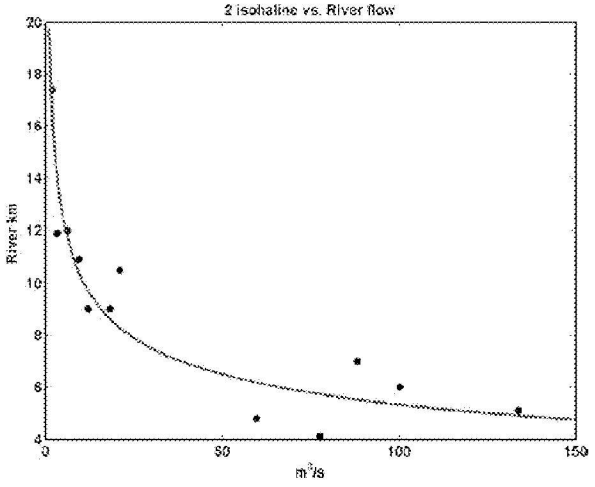

Fig. 9 Position of 2 psu isohaline based on CTD surveys of the river. Note that the surveys were all began approximately 2 h after high water because of navigational needs associated with low bridges around km 7. The *blue line* is the best fit based on river discharge which was proportional to $Q^{-0.28}$

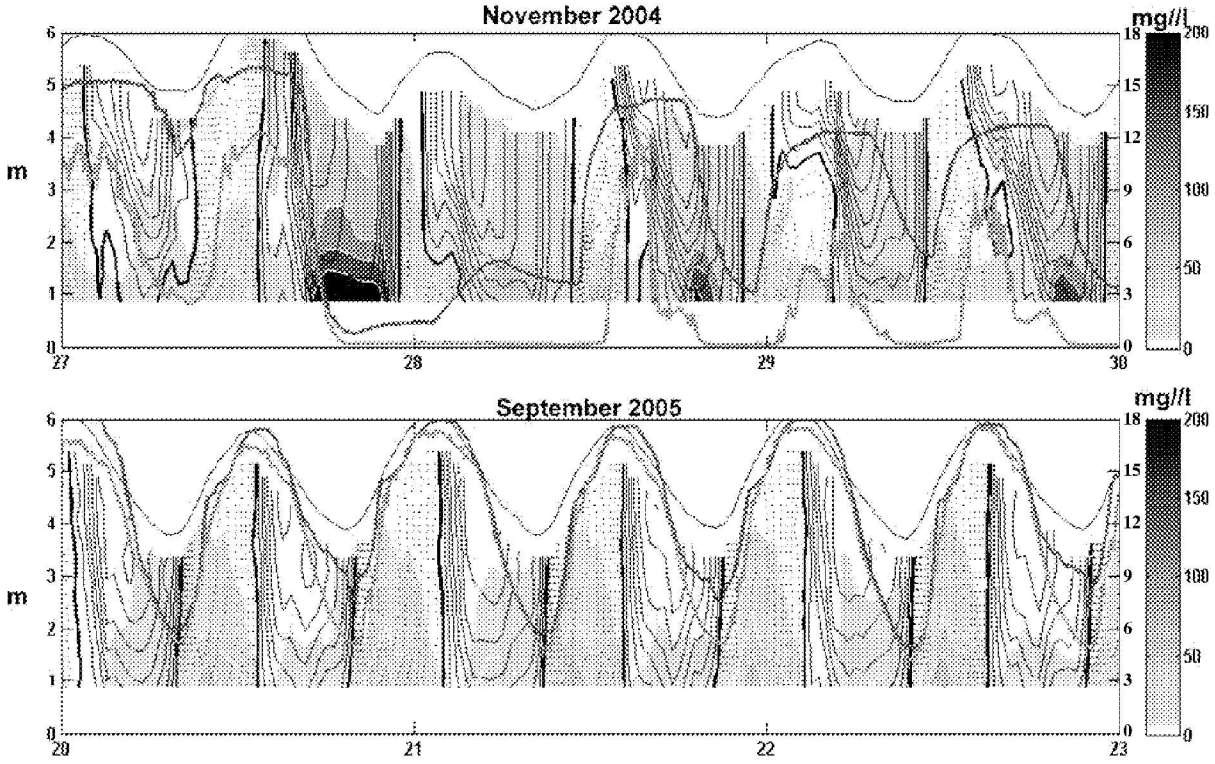

Fig. 10 Times series from mooring M2 during high flow (Q ~100 m^3/s) and low flow Q=2 m^3/s) from November 2004 to September 2005, respectively. *Color* and *white contours* are total suspended sediment from ADCP backscatter calibrated against TSS measurements. *Black contours* are along channel velocity at 10 cm/s intervals. *Thick black contour* is the zero isotach, *dashed lines* indicate flooding currents, and *solid lines* are ebbing currents. *Red* and *blue lines* are surface and bottom salinity with salinity values indicated on *right axis*

during July 2005, when river discharge was around 5 m^3/s TSS levels are lower, the tidal asymmetry is reversed though not as pronounced with only modestly elevated TSS on the flood. The water column is well mixed for much of this time; however, vertical salinity stratification develops during the weaker evening ebb tide and TSS levels are generally suppressed relative to the stronger morning ebb.

Sediment Transport

Decomposition

To quantify the relative role of tides and river discharge in driving sediment transport processes, we estimated the sediment flux with the moored ADCP data and decomposed these fluxes into a riverine, estuarine, and tidal component. This analysis is analogous to the salt flux decomposition described in Lerczak et al. (2006) or sediment flux decompositions (Dyer 1988; Jay et al. 1997). We note that this estimate neglects lateral variability in sediment transport which will modify these results.

The instantaneous total sediment transport flux per unit width, $\Im_{TSS}$, is the vertical integral of the product of $U \times$ TSS, i.e.

$$\Im_{TSS} = \int_0^{\eta} U \times C \partial z \tag{1}$$

where U is the along channel current velocity, C is the total suspended sediment concentration obtained from the acoustic backscatter from the ADCP, and z is the vertical coordinate. The integral is taken from the bed to the sea surface (η). To include the near surface and near bottom portions of the water column not covered by the ADCP, profiles were extrapolated. Velocity data in the bottom meter of the water column were extrapolated assuming a log profile, i.e.,

$$u(z) = \frac{u_*}{\kappa} \ln\left(\frac{z}{z_0}\right) \tag{2}$$

where u_* is the bottom friction velocity, κ is von Karman's constant (0.4), and z_0 is the bottom roughness, which we take as 0.067 m (Lerczak et al. 2006). We note that results are relatively insensitive to details of the choice of z_0. The

fit is obtained by fitting a log profile to the three bottom ADCP bins and assuming that the velocity is zero at z_0. Velocity profiles near the surface are extrapolated assuming that the vertical shear linearly decrease from the observed shear at the top of the profile to zero shear at the surface. Vertical shear at the top of the ADCP profile is obtained by linear regression to the upper three velocity measurements. Both near surface and near bottom TSS levels were obtained by linear extrapolation. While we could have used a Rouse profile to estimate TSS levels near the bottom, we felt that given the time dependent nature of the TSS field that the use of an exponentially increasing sediment concentration near the bottom could potentially lead to significant overestimate of near bottom TSS levels.

With the extrapolated profiles, we then transformed the vertical coordinate system in to a sigma (σ) coordinate system. The use of the σ coordinate system provides a continues time series at all σ levels which is in contrast to the z-coordinate system (i.e., fixed ADCP bins) where the upper bins (z levels) move in and out of the water column with the tidally varying sea level. The use of the σ-coordinate system enables filtering of the near surface data which is required to decompose both velocity and suspended sediment into tidal and subtidal components. The σ-coordinate system is defined as:

$$\sigma = \frac{z-\eta(t)}{h+\eta(t)} \tag{3}$$

where h is the mean water column depth and $\eta(t)$ is the time dependent sea level which varies at tidal and subtidal time scales. Each profile of along channel velocity and suspended sediment concentration was interpolated to 51 equally spaced grids in σ space. Next both the along channel velocity and TSS were decomposed into three components to represent processes associated with river flow (U_R, C_R), estuarine circulation (U_e, C_e), and the higher frequency tidal currents (U_I, C_I). To perform this decomposition, we first filter each σ level time series of along channel current velocity and suspended sediment concentration with a low-pass filter utilizing a Lanczos window with a half power cut-off of 32 h to produce low-passed records $U_{LP}(t,\sigma)$ and $C_{LP}(t,\sigma)$. The river flow time series $U_r(t)$, $C_r(t)$ are the vertical average of $U_{LP}(t,\sigma)$ and $C_{LP}(t,\sigma)$, which thus are only functions of time. The estuarine circulation terms U_e, C_e are the difference between the low-passed data and U_r, C_r, i.e.,

$$\begin{aligned} U_e(t,\sigma) &= U_{lp}(t,\sigma) - U_r(t) \\ C_e(t,\sigma) &= C_{lp}(t,\sigma) - C_r(t) \end{aligned} \tag{4a, b}$$

Finally, tidal period variability (U_T, C_T) was isolated by subtracting the low-passed filtered signal from the raw data (i.e., $U_T(t,\sigma)=U(t,\sigma)-U_{lp}(t,\sigma)$). With these time series, we are able to construct time series of sediment transport that are driven by the river discharge ($\Im_r$), estuarine circulation ($\Im_e$), and by tidal pumping ($\Im_T$) and are defined by:

$$\Im_r(t) = HU_rC_r \tag{5a}$$

$$\Im_e(t) = H\int_0^1 U_eC_e\partial\sigma \tag{5b}$$

$$\Im_T(t) = H\int_0^1 U_TC_T\partial\sigma \tag{5c}$$

where $U_r = \int_0^1 U_{lp}\partial\sigma$ and $C_r = \int_0^1 C_{lp}\partial\sigma$ and $H = (h+\eta)$ and the overbar in Eq. 5c indicates low-passed filtering because we are interested in sediment transport processes at subtidal periods.

Figure 11a, b shows the result of this analysis for each of the three mooring deployments. During times of moderate to high river discharge (Fig. 12a), the mean outflow drives sediment out of the river and, as expected, this transport increases markedly with river flow. Also, during time of high river discharge the tidal pumping term drives sediment out of the Passaic. The enhancement of seaward tidal pumping during times of high river discharge occurs for two reasons. First, river flows are sufficient in this reach to significantly increase ebb velocities and reduce flood velocities. This produces large near bottom stresses on the ebb which drives ebb tide resuspension events. Secondly, at moderate to high river flow events the salt front is at times downstream of the Harrison Reach and thus there is no stratification to inhibit turbulent mixing thus increasing sediment transport particularly during the ebb when the tidal current augments river discharge. Also note that during times of high river flows the landward estuarine sediment transport also increases because the vertical structure in both the mean velocity and TSS are enhanced. However, the contribution of sediment transport due to the mean shear is significantly smaller than the contribution due to tidal pumping and river discharge, and thus during times of moderate to high river flow net sediment transport is seaward. This is evident during the second half of the first deployment and most of the second deployment when the mean river discharge was often high (not shown). Peak sediment transport during the high flow events was approximately 0.05 kg/ms, which if were representative the channel cross section would represent approximately 10 kg/s or approximately 400 metric tons per day. Similar sediment flux rates and phenomenology were also apparent during the second deployment when river flow was also

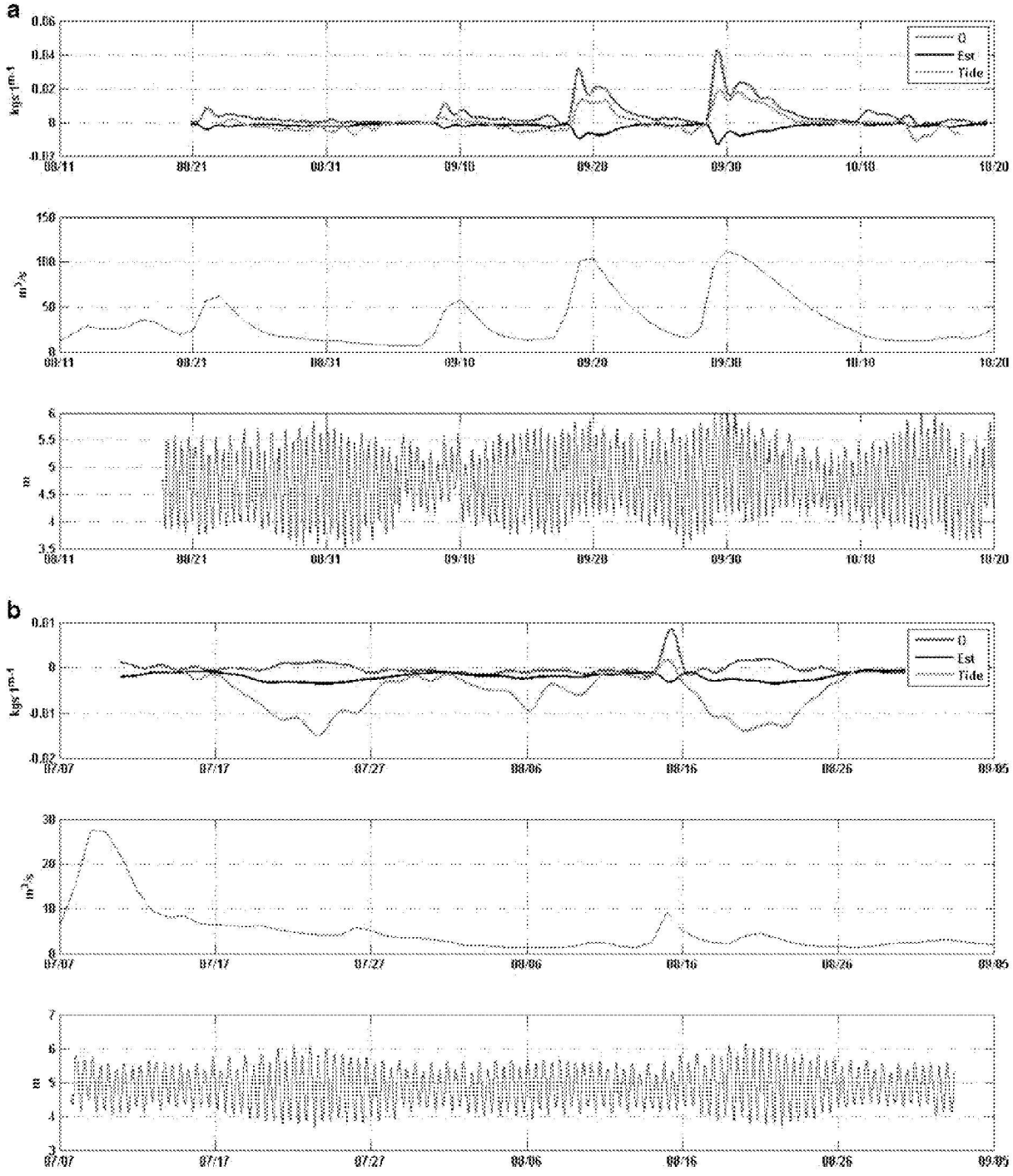

Fig. 11 **a** *Upper panel* shows sediment flux decomposition as described by Eq. 5a–c during the first mooring deployment which was characterized by relatively high river discharge. *Blue line* is the river transport term, *black* is the estuarine transport term, and *red* is the tidal pumping term. *Middle panel* shows river discharge and *lower panel* shows sea level elevation. **b** *Upper panel* shows sediment flux decomposition as described by Eq. 5a–c during the third mooring deployment which was characterized by low river discharge. *Blue line* is the river transport term, *black* is the estuarine transport term, and *red* is the tidal pumping term. *Middle panel* shows river discharge and *lower panel* shows sea level elevation

high and sediment flux was primarily seaward and dominated by tidal pumping and river flow (not shown).

During the third mooring deployment, the mean river flow was less than 5 m^3/s and the net sediment transport was dominated by tidal pumping. Moreover, the tidal pumping term is up river and strongly modulated over the spring neap cycle with enhanced tidal pumping during spring tides. However, the magnitude of this term is approximately an order of magnitude less than during high flow conditions. During the low flow sediment flux is directed upstream at 12 kg/s during spring tides corresponding to a daily flux of approximately 100 metric tons per day.

The dominance of the high discharge event was clearly evident during the discharge event on April 4–5, 2005 when the daily mean river discharge peaked was 330 m^3/s on both days. Unfortunately, we did not have mooring in during this time but river discharge was sufficient to arrest the flood tide. A shipboard survey on April 5 around maximum ebb indicated that depth averaged TSS levels in the river were around 250 mg/l (Fig. 8). Note that to achieve a level of 250 mg/l solely from local resuspension requires the mobilization of 2 cm sediment assuming a mean channel depth of 4 m and a dry sediment weight of 600 kg/m^3. However, since much of this sediment is likely from an upstream source, this represents an upper bound on the local resuspension.

Assuming that the sediment transport out of the river is equal to the observed TSS level (250 mg/l) times the river discharge and that this transport is only active during the ebb phase of the tide suggests a daily sediment flux of over 3,000 metric tons per day, corresponding to a net sediment flux over this 2-day event of approximately one fourth of the annual sediment loadings to the Passaic River (Steinberg et al. 2004). While this event transported a large load of sediment to Newark Bay, it was followed by a dry period that coincided with the 2005 mooring deployment during which time there was a net upstream transport of sediment. More generally the data emphasizes large episodic downstream sediment transport events during high flow that are followed by weaker but more persistent upstream sediment transport during low flow events. Together, these two phases of sediment transport processes act to homogenize the sediments in this system.

To concisely summarize the above results, we developed an empirical model that related sediment transport rates to tidal range and river discharge. With the moored data, we estimated a daily net sediment transport rate and binned these results as a function of tidal range and river discharge (Fig. 12). During low flow condition, defined by flows less than 30–40 m^3/s, there is net landward sediment transport that has a maximum value of approximately 100 metric tons per day during spring tides with near zero river flows.

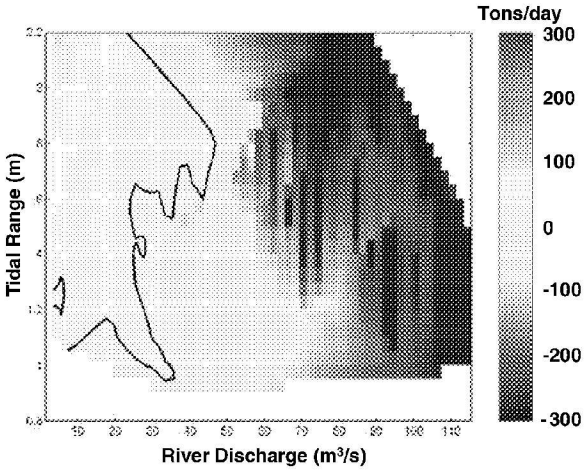

Fig. 12 Daily net sediment transport binned as a function of river discharge and tidal range. *Yellow* to *red colors* represent upriver transport and *blue colors* represent down river transport. *Thick black line* represents zero net transport

In contrast, a net downstream sediment transport of over 300 metric tons per day occurs during high river discharge over a range of tidal forcing. While there is some spring neap variability apparent in this figure, particularly during the low flow condition (likely due to the higher density of data in the low flow regime), most of the variability is associated with variations in river discharge.

With most of the variance in sediment transport determined by river discharge, we collapse the data from Fig. 12 by averaging across tidal range and plot mean daily sediment transport as a function of river discharge (Fig. 13), indicating a power law relationship between river discharge and net sediment transport. The red line is a fit to the data based on a second order polynomial. This plot indicates the steep increase in sediment transport for high flow conditions and includes the crude estimate of 3,000 tons per day made with the CTD section during the high flow event on April 5, 2005. Note that during low flow conditions, there is a net upstream sediment flux while during high flow events net flux is downstream.

Applying the above fit to daily Passaic River discharge data from 1980 to 2008 and averaging over each year, we estimated the annual net sediment transport past the Harrison Reach (Fig. 14; We note that channel depth was deeper in the early part of this record—which would reduce net downstream sediment fluxes in the early part of the record and we comment on this later). Due to variability in river discharge from year to year, there is a large variability in the magnitude and even the sign of the net sediment transport. In five of the years (1981, 1985, 1988, 1995, and 2002), there was a net upstream sediment transport due to low river discharges those years. The maximum down-

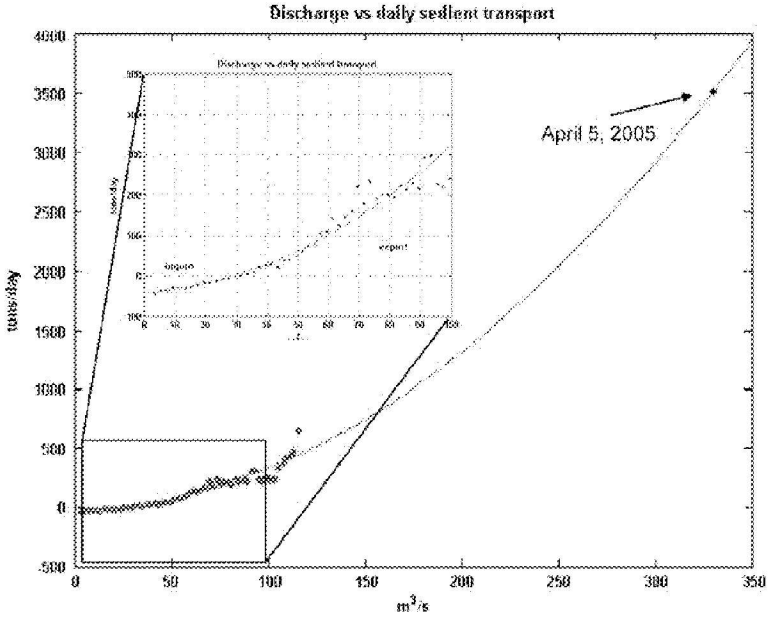

Fig. 13 Daily net sediment transport (Tf; *y*-axis) only as a function of river discharge (*x*-axis). The *insert* is zoomed in at low river flow events to emphasize zero crossing at a river flow of around 30 m^3/s. Included in the figure is the rough estimate from the high flow event on April 5, 2005. *Red line* is best fit for a second order polynomial relating sediment flux to river discharge. The fit is $Tf=-41+0.052\times Q+0.0031\times Q^2$, where Q is the mean daily freshwater discharge in cubic meter per second

stream transport occurred in 1984 with a net flux of 66,000 tons, due to three large discharge events, the largest which contributed nearly 60% of the net annual flux. The mean value over this period is 18,000 tons/year with a standard deviation of 20,000 tons/year.

Historical Infilling of the Passaic and Implications for 2,4,7,8 TCDD Trapping

The high sediment deposition noted by Huntley et al. (1995) is also apparent in a comparison of channel depths from historic navigational charts from and recent high resolutions bathymetric surveys (Fig. 15). Moreover, this comparison reveals that the Passaic's channel has been accreting seaward since dredging ceased in the 1940s. Between 1940 and 1960 the highest deposition, according to the depths reported on the navigational charts, occurred between river km 2–4, coinciding with the Harrison Reach, while between 1960 and 1980 the highest accumulation rates occurred closer to the mouth around km 1 and depths from a more detailed 2000 survey indicates that while the channel is continuing to shoal it is also approaching the depths from the 1835 survey. This suggests that the river is approaching geomorphological equilibrium. Moreover, the continual decrease in cross-sectional area along the Passaic (see Fig. 1) is consistent with that needed for an "equilibrium" tide whereby tidal velocity amplitude are relatively uniform along the estuary and further long-term deposition is no longer favored (Friedrichs 2010).

A crude estimate of the total sediment trapped in this lower 10 km over the past 60 years is close to the total sediment loadings to the River. Figure 15 indicates that total deposition over the past 60 years is 0–2 m at km 10 and nearly 5 m in the lower reaches. Thus the total volume of sediment accumulated over this reach, taking the mean width of 120 m, is 3.6×10^6 m^3. The wet density of sediment in the Passaic has been reported to be ~1,250 kg/m^3 which corresponds to a dry weight of ~600 kg/m^3. Thus this volume of sediment corresponds to 2.1 million tons of

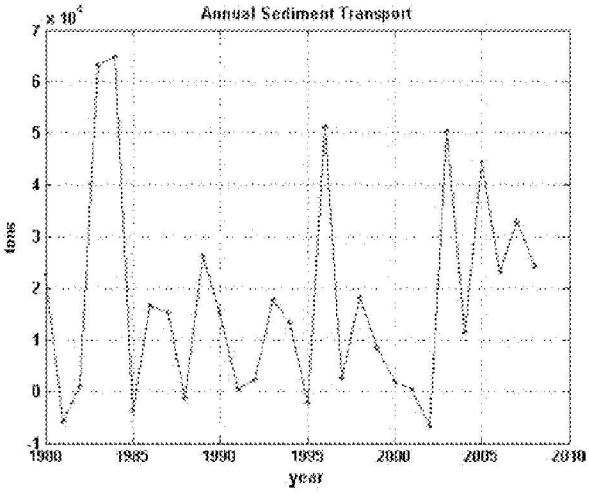

Fig. 14 Annual net sediment flux based on fit from Fig. 13 applied to daily discharge data and integrated annually. *Positive values* represent a net sediment flux out of the river while *negative values* represent an upriver transport

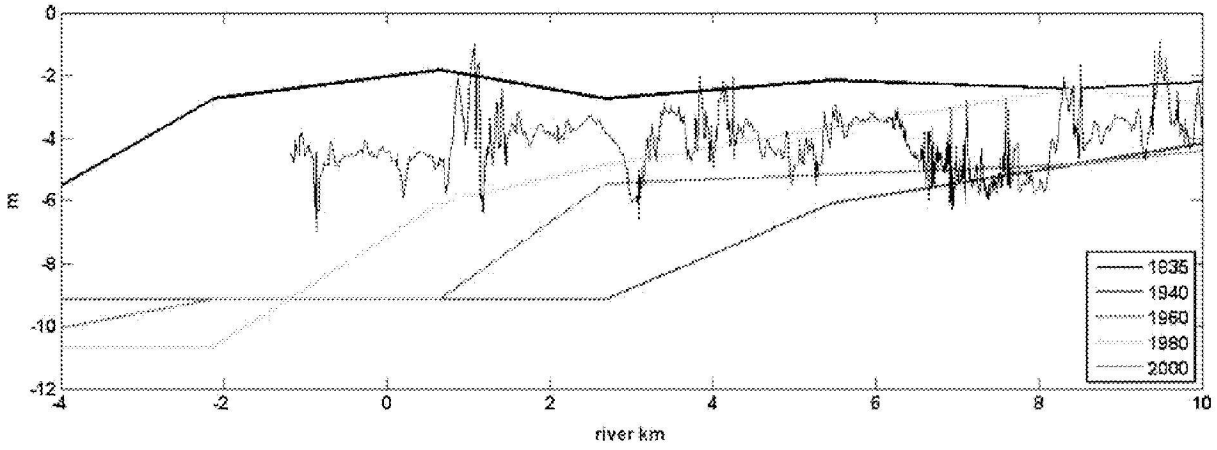

Fig. 15 Channel depths based on historical NOAA Charts (*thick lines*) and from 2000 USGS survey (*thin line*)

sediment or an annual average of 36,000 tons per year which actually exceeds estimates of the net sediment input into the Passaic River. This indicates that the Passaic has been a highly efficient sediment trap over the past 60 years, potentially importing sediments from Newark Bay. The historically high trapping efficiency of the Passaic is supported by Bopp et al. (1991) who concluded that 4–8 kg of dioxin were released from the Passaic into Newark Bay over this period compared to the 40–50 kg that have been estimated to be trapped in the sediment within the river.

It is well-known that estuaries are effective sediment traps (Geyer 1993; Dyer 1988). Observations presented here indicate that the Passaic River tends to trap sediment only when river discharge is below 50–100 m^3/s. Above this discharge, the estuarine length becomes less that a tidal excursion allowing sediment to be discharged from the estuary during the ebb tide and that these short-lived events dominate the more persistent upstream events that occur during low flow conditions. However, when the channel was deeper, the estuary was more efficient trap because the salt front penetrated further up river than it does today. The length of salt intrusion, L_x, is related by channel depth, H; width, W; tidal current amplitude, U; and river discharge, Q, by the relationship (Ralston et al. 2008; Monismith et al. 2002)

$$L_x \sim \frac{W^{1/3}H^2}{Q^{1/3}U} \tag{6}$$

Note that in using the expression in Ralston et al. (2008), we have replaced the river cross-sectional area with product WH. In addition to the depth changing, we also expect the tidal current amplitude to change inversely proportional to channel depth. Because the Passaic's channel is short compared to the tidal wavelength, the tidal currents can be approximated with continuity alone, i.e.,

$$U = \frac{A_s \eta_o \omega}{\mathrm{WH}} \tag{7}$$

Where A_s, η_o, and ω are the estuarine surface area, tidal amplitude, and frequency, respectively. Thus assuming that the tidal amplitude remained the same, we expect the salt

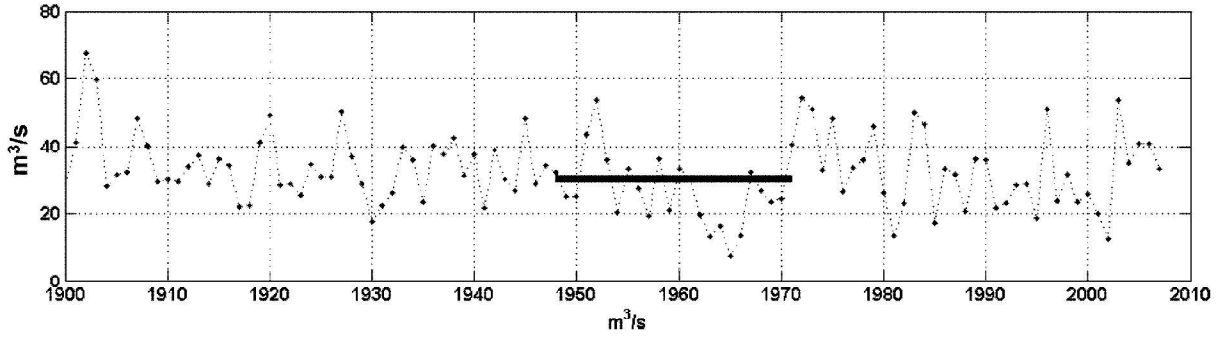

Fig. 16 Mean annual river discharge from 1900 to 2008. *Thick solid line* depicts time period that Agent Orange was manufactured along the Harrison Reach near mooring M2

water intrusion length to increase with the *cube* of the channel depth.

Thus in the 1940s when the channel depth was over two times than what it is today, Eqs. 6 and 7 suggest that the salt field may have extended up to eight times further up river than it does today. While this is probably an overestimate since the upriver section was not as deep and the significant shoaling has only occurred in the lower 10 km, it seems likely that the salt field in the Passaic River during the time that Agent Orange was manufactured resided much further up river and allowed the Passaic to trap most of the dioxins that were released into the river. The increased depth and decreased tidal velocities are likely to have further enhanced local deposition as a result of reduced bottom stresses and reduced resuspension, favoring a return to shallower depths and higher velocities at equilibrium (Friedrichs 1995). Also contributing to the trapping of dioxins in the river may have been climatic variability. In particular, river flows were generally low during the time that Agent Orange was manufactured in the river (Fig. 16) especially during the severe drought between 1962 and 1966. Indeed during this 5-year period there were only two events when discharge exceeded 100 m^3/s with a maximum discharge of only 138 m^3/s occurring on March 15, 1962. Given the deeper channel depths then, we suggest that during this 4-year period the salt wedge was probably never advected out of the system and that there was a persistent trapping of sediments and associated contaminants during this period.

Conclusions

This paper reports the first comprehensive characterization of the dynamics and associated sediment transport processes of the Passaic River. Since dredging of the river ceased in the 1950s, the channel has been highly depositional (Huntley et al. 1995) accumulating both sediments and contaminants in the lower reaches of the system, though some of these contaminants have escaped to the adjacent waters and continue to do so today (Bopp et al. 1991; Powers et al. 2006). Moored data showed that the tidal asymmetries both in depth averaged currents and in the vertical structure of the tidal currents tend to favor landward sediment flux. However, the salt field is washed out of the system for river discharges over 100 m^3/s and these episodic events appear to overcome the more persistent but weaker upstream fluxes resulting in a net export of sediment from the Passaic to Newark Bay. By fitting a power curve of sediment flux to river discharge, we estimate that the mean sediment flux leaving the river (at the Harrison Reach) is approximately equal to estimates of annual loadings to the system, suggesting that the channel is approaching geomorphological equilibrium. This is also suggested by historical navigational charts and recent bathymetric surveys that reveal the evolution of the channel back towards its pre-dredging channel depths based on an early 19th navigational chart.

These bathymetric changes in the Passaic River over the past 60 years have significantly altered its ability to trap sediments and contaminants. This is consistent with the fact that most of the dioxins released to the River appear to be trapped within the channel with less than 20% released to the adjacent water ways. It also is consistent with a simple scaling analysis that suggests that the salt water intrusion length, and thus the ability to trap sediment, scales with the cube of the channel depth. Thus the factor of 2 change in the channel depth over the past 60 years corresponds to a factor of 8 change in the salt intrusion length. Moreover, severe droughts in the 1960s when Agent Orange was manufactured facilitated the trapping of these contaminants in the system. We suggest that between 1962 and 1966 the salt wedge remained well upstream of the Harrison Reach and during this time the system was a highly effective trap of particle bound contaminants released into the system.

While the river appears to have approached morphological equilibrium, we do not know if the sediment that leaves the estuary is simply clean sediment that enters upstream or a combination of relic contaminated sediment and clean sediment. In particular, more detailed measurements of contaminated concentration on suspended sediment need to be made during high discharge events. For example, is the suspended load more contaminated during high flow events, suggestive of the release of relic sites, or is it less contaminated, suggestive of clean sediment bypassing the system during such events? While attempts to make such measurements were undertaken during the New York/New Jersey Contaminant Assessment and Reduction Program, the program in the Passaic unfortunately occurred during a drought in 2001–2002 and was unable to capture an extreme discharge event. Finally, of critical importance to remediation strategies is determining the stability of the river bed to large discharge events, such as the 1903 flood that approached 800 m^3/s. The 2005 event, where discharge was 300 m^3/s that we described here, revealed mean suspended loads of approximately 250 g/m^3 suggestive that sediment resuspension was up to 2 cm of the bed. However, given the high power law dependence of resuspension (Winterwerp 2001), more work on sediment stability is clearly warranted.

Acknowledgments This work was funded by a grant from the New Jersey Department of Transportation. We are grateful for the dedicated work of Elias Hunter and Chip Haldeman who lead the mooring efforts and for Tim Wilson for running the TSS samples. We also thank Carl Friedrichs for his thorough, insightful and constructive criticism of an earlier draft of this manuscript.

References

Bopp, R.F., M.L. Gross, H. Tong, H.J. Simpson, S.J. Monson, B.L. Deck, and F.C. Moser. 1991. A major incident of dioxin contamination: sediments of New Jersey estuaries. *Environmental Science & Technology* 25(5): 951–956.

Chant, R.J., and R.E. Wilson. 2000. Internal hydraulics and mixing in a highly stratified channel. *Journal of Geophysical Research* 105 (C6): 14215–14222.

Dyer, K.R. 1986. *Coastal and estuarine sediment dynamics*. Chichester: John Wiley & Sons.

Dyer, K. 1988. *Fine sediment particle transport in estuaries*, 295–310. Springer-Verlag: Physical Processes in Estuaries. D. a. v. Leussen.

Friedrichs, C. 1995. Stability shear stress and equilibrium cross-sectional geometry of sheltered tidal channels. *Journal of Coastal Research* 11(4): 1062–1074.

Friedrichs, C. (2010). Barotropic tides in channelized estuaries. In Contemporary issues in estuarine physics, ed. Valle-Levinson, 27–61. Cambridge England: Cambridge University.

Friedrichs, C.T., and D.G. Aubrey. 1988. Non-linear tidal distortion in shallow well-mixed estuaries: a synthesis. *Estuarine, Coastal and Shelf Science* 27: 521–545.

Friedrichs, C.T. and D.G. Aubrey. 1995. Uniform bottom shear stress and equilibrium hypsometry of intertidal flats. In Mixing processes in estuaries and coastal seas, ed. C. Pattiaratchi, 1–25. Washington, D.C.: American Geophysical Union.

Geyer, W.R. 1993. The importance of suppression of turbulence by stratification on the estuarine turbidity maximum. *Estuaries* 16(2): 113–125.

Geyer, W.R., J.H. Trowbridge, and M.M. Bowen. 2000. The dynamics of a partially mixed estuary. *Journal of Physical Oceanography* 30: 2035–2048.

Hansen, D.V., and M. Rattray. 1966. New dimensions in estuary classification. *Limnology and Oceanography* 11: 319–326.

Huntley, S.L., R.J. Wenning, S.H. Su, N.L. Bonnevie, and D.J. Paustenbach. 1995. Geochronology and sedimentology of the lower Passaic River, New Jersey. *Estuaries* 18(2): 351–361.

Jay, D.A., and J.D. Musiak. 1993. *Internal tidal asymmetry in channel flows: origins and consequences*. Washington DC: American Geophysical Union.

Jay, D., W. Geyer, R. Uncles, J. Vallino, J. Lagier, and W. Boynton. 1997. A review of recent developments in estuarine scalar flux estimation. *Estuaries* 20(2): 262–280.

Klingbeil, K.D., and C.K. Sommerfield. 2005. Latest Holocene evolution and human disturbances of a channel segment in the Hudson River Estuary. *Marine Geology* 218: 135–153.

Lerczak, J.A., W.R. Geyer, and R.J. Chant. 2006. Mechanisms driving the time-dependent salt flux in partially stratified estuary. *Journal of Physical Oceanography* 36(12): g2283–2298.

Lurie, N.M. and M. Mappen. 2004. Encyclopedia of New Jersey, Rutgers University Press.

MacCready, P. 1999. Estuarine adjustment to changes in river flow and tidal mixing. *Journal of Physical Oceanography* 12: 708–726.

MacCready, P. 2004. Toward a unified theory of tidally-averaged estuarine salinity structure. *Estuaries* 27(4): 561–570.

Monismith, S.G., W. Kimmerer, J.R. Burau, and M.T. Stacey. 2002. Structure and flow-induced variability of the subtidal salinity field in northern San Francisco Bay. *Journal of Physical Oceanography* 32(11): 3019–3032.

Powers, C.W., G.R. Munoz, and R.A. Panero. 2006. Pollution prevention and management strategies for dioxins in the New York/New Jersey Harbor. New York Academy of Science, New York: 259.

Ralston, D.K., W.R. Geyer, and J.A. Lerczak. 2008. Subtidal salinity and velocity in the Hudson River estuary: observations and modeling. *Journal of Physical Oceanography* 38 (4): 17.

Steinberg, N., D.J. Suszkowski, L. Clare, and J. Way. 2004. Health of the Harbor: the first comprehensive look at the state of the NY/NJ Harbor estuary. N. Y. N. J. H. E. Program. New York City: 86.

Winterwerp, J.C. 2001. Stratification effects by cohesive and non-cohesive sediment. *Journal of Geophysical Research* 106: 22,559–22,574.